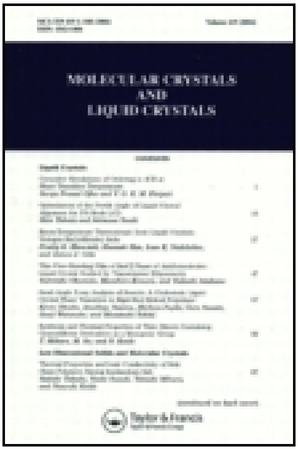

Molecular Crystals and Liquid Crystals Science and Technology. Section A. Molecular Crystals and Liquid Crystals

Publication details, including instructions for authors and subscription information:
http://www.tandfonline.com/loi/gmcl19

Electromagnetic Wave Propagation in Twist Grain Boundary Phases

Pascal Hubert [a], Marta Becchi [a] & Claudio Oldano [a]

[a] Dipartimento di Fisica del Politecnico di Torino and, Istituto Nazionale di Fisica della Materia, Corso Duca degli Abruzzi 24, 10129, Torino, Italy

Version of record first published: 24 Sep 2006

Mol. Cryst. Liq. Cryst., 1999, Vol. 328, pp. 57-64
Reprints available directly from the publisher
Photocopying permitted by license only

Electromagnetic Wave Propagation in Twist Grain Boundary Phases

PASCAL HUBERT, MARTA BECCHI and CLAUDIO OLDANO

Dipartimento di Fisica del Politecnico di Torino and Istituto Nazionale di Fisica della Materia, Corso Duca degli Abruzzi 24, 10129 Torino, Italy

The propagation of electromagnetic waves within Twist Grain Boundary samples are theoretically considered. Fully analytical expressions for light propagating along the superstructure helix axis are given. The optical properties for oblique light are studied numerically. Moreover, an homogeneous model is developed for pitch shorter than the wavelength in order to describe the natural optical activity. The possibility to obtain the material parameters by optical methods is discussed.

Keywords: TGB phase; Bragg reflection; optical activity

INTRODUCTION.

The theoretical works of de Gennes [1] and Renn-Lubensky [2,3], concerning the analogy between the smectic phase and the Abrikosov phase in type II superconductor, gave the first contribution to the discovery of TGB phases. Actually, three types of phase referred as TGBA [4], TGBC [5] and TGBC* [6] are known. The first two are constituted by a set of homogeneous SmA and SmC slabs, respectively, separated by inhomogeneous transition layers. The last one presents a double periodic structure and will not be considered here. In Fig.1 the structure of the TGBA phase, confirmed by many experiments [7] is shown. Two successive smectic slabs of thickness l_b are rotated by an angle $\Delta\varphi$ around a direction parallel to the smectic planes, say z. The transition layer contains a set of regularly spaced screw dislocation lines. In general, its thickness is optically negligible. Therefore, the whole sample can be treated as a set of homogeneous slabs of thickness l_b, separated by

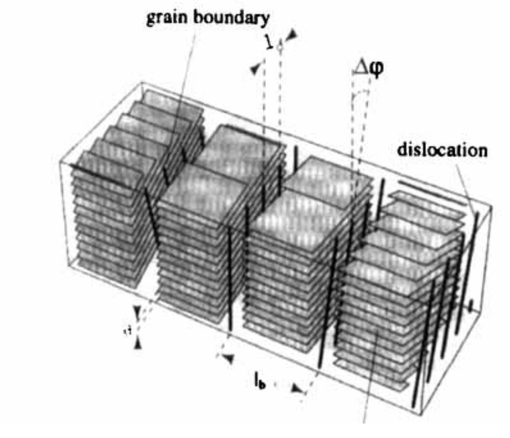

Fig. 1. Schematic representation of TGB phase.

planes of discontinuity (grain boundaries). This gives a helix-like superstructure similar to the cholesteric one, with the difference that the rotation of the local optic axis is discontinuous. The structure of the TGBC phases can be different because the slabs are biaxial and the nematic director can be, at least in principle, obliquely oriented with respect to the helix axis. However, the director of the experimentally discovered TGBC phases is orthogonal to the helix axis and the biaxiality is small: their optical properties are therefore practically the same as for the TGBA phases [8].

The aim of this paper is to study the optical properties of the TGB phases in order to get their structural parameters. To this purpose, we consider the transmission and the reflection properties of samples whose superstructure helix axis is orthogonal to the sample boundaries. We also show that the optical properties of short pitch sample are well approximated by an effective homogeneous medium. The starting point of our analysis is the Berreman equation [9]

$$\frac{\partial\beta}{\partial z} = ik_0 B\beta, \qquad (1)$$

where $\beta = \left(E_x, H_y, E_y, -H_x\right)^t$ (t for transpose), $k_0 = \frac{2\pi}{\lambda}$ and B is the Berreman matrix. It is convenient to define within each layer an α-vector, whose components are the amplitudes of the four propagating plane waves (two forward and two backward). This vector is given by $\beta = T\alpha$, where T is the 4x4 matrix whose element t_{ij} is the i^{th} component of the eigenvector β^j of the Berreman matrix. The propagation matrix for the α-vectors is $U_\alpha = T^{-1}U_\beta T$, where U_β is the propagation matrix for the Berreman β-vector, defined by the relation $\beta(z)=U_\beta(z)\beta(0)$.

NORMAL INCIDENCE.

Let us consider a plane wave normally incident on a set of N homogeneous slabs which are between N+1 planes at $z=z_n=nl_b$ $(n=0,1,\dots,N)$. The continuity of the tangential components of the vectors **E** and **H** is written as $\beta(z_n^+)=\beta(z_n^-)$ and it gives

$$\alpha(z_n^+)=T_n^{-1}\,T_{n-1}\,\alpha(z_n^-), \qquad (2)$$

where T_{n-1}, T_n are the T-matrices of the layers (n-1) and (n), respectively. The transfer matrix for the α-vectors between the planes $z=z_{n-1}^-$ and $z=z_n^-$ (corresponding to the n-layer and its first interface) can be written as

$$U_n = P_n\,R_{n,n-1}, \qquad (3)$$

with $R_{n,n-1}=T_n^{-1}\,T_{n-1}$ and P_n is the diagonal transfer matrix for the n^{th} homogeneous slab. The elements of P_n are $\exp(ik_0n_jl_b)$, $(j=1,\dots,4)$, where n_j are the eigenvalues of the Berreman matrix B_n. At normal incidence, P_n is independent of the index n and $n_j=\pm n_e, \pm n_o$; where n_e, n_o are the extraordinary and ordinary refraction indices of the smectic slabs, assumed as uniaxial. From Ref.10, the matrices T_n and $R_{n,n-1}$ are easily found as follow

$$T_n=\begin{pmatrix} \dfrac{\cos\varphi_n}{\sqrt{n_e}} & \dfrac{\cos\varphi_n}{\sqrt{n_e}} & -\dfrac{\sin\varphi_n}{\sqrt{n_o}} & -\dfrac{\sin\varphi_n}{\sqrt{n_o}} \\ \cos\varphi_n\sqrt{n_e} & -\cos\varphi_n\sqrt{n_e} & -\sin\varphi_n\sqrt{n_o} & \sin\varphi_n\sqrt{n_o} \\ \dfrac{\sin\varphi_n}{\sqrt{n_e}} & \dfrac{\sin\varphi_n}{\sqrt{n_e}} & \dfrac{\cos\varphi_n}{\sqrt{n_o}} & \dfrac{\cos\varphi_n}{\sqrt{n_o}} \\ \sin\varphi_n\sqrt{n_e} & -\sin\varphi_n\sqrt{n_e} & \cos\varphi_n\sqrt{n_o} & -\cos\varphi_n\sqrt{n_o} \end{pmatrix}, \qquad (4)$$

$$R_{n,n-1}=\begin{pmatrix} \cos\Delta\varphi & 0 & A\sin\Delta\varphi & B\sin\Delta\varphi \\ 0 & \cos\Delta\varphi & B\sin\Delta\varphi & A\sin\Delta\varphi \\ -A\sin\Delta\varphi & B\sin\Delta\varphi & \cos\Delta\varphi & 0 \\ B\sin\Delta\varphi & -A\sin\Delta\varphi & 0 & \cos\Delta\varphi \end{pmatrix}, \qquad (5)$$

where $\Delta\varphi=\varphi_n-\varphi_{n-1}$, $A+B=\sqrt{n_e/n_o}$ and $A-B=\sqrt{n_o/n_e}$. Since both the angle $\Delta\varphi$ (between the optical axis of two successive slabs) and the slab thickness l_b are independent of n, all the matrices U_n are identical and equal to $U_1=R_{1,0}\,P_0$. The properties of the whole sample are then governed by the properties of the matrix U_1, and more precisely by its eigenvalues u_j and eigenvectors α_j: a set of N slabs has the same eigenvectors α_j and the eigenvalues u_j^N. It is easy to found that the eigenvalues occur in pairs u and 1\u. This allows to write the characteristic equation as [11]

$$g(y) = y^2 + 2ay + b \qquad (6)$$

where $y = u + 1/u$, $a = 2\cos\Delta\varphi \sin(\Delta\phi/2)\sin\phi$ and

$$b = 2(1+\cos^2\Delta\varphi)[\cos^2\phi + \cos^2(\Delta\phi/2)] + \left(\frac{n_e}{n_o} + \frac{n_o}{n_e}\right)\sin^2\Delta\varphi\,[\cos^2\phi - \cos^2(\Delta\phi/2)] - 4,$$

with $\phi = k_0 l_b \tilde{n}$ and $\Delta\phi = k_0 l_b \Delta n$ where $\tilde{n} = (n_o + n_e)/2$ and $\Delta n = n_e - n_o$. The quantities $l_b \tilde{n}$ and $l_b \Delta n$ are the mean optical path and the optical path difference between the ordinary and extraordinary waves within each slab. It is convenient to set $u_j = \exp(ik_j l_b)$, where k_j plays the role of an effective wavevector for the periodic medium. Therefore, a real k corresponds to a propagating wave (*stable solution*) and a complex or purely imaginary k to an evanescent one (*unstable solution*).

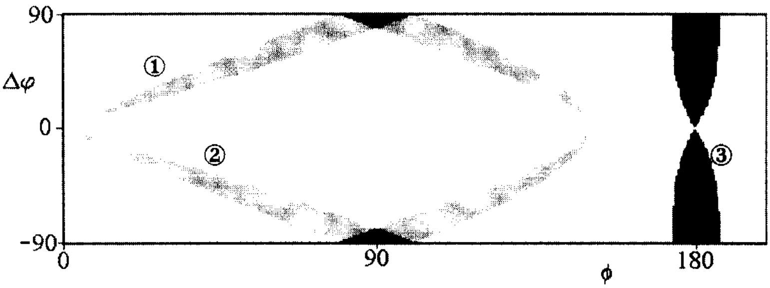

Fig.2: Chart of stability at normal incidence with n_e=3 n_o=2. White, gray and black regions correspond to the cases where there are four, two and zero propagating waves, respectively.

A typical chart of stability is shown in Fig.2. The white, gray and black regions correspond to the cases where there are four, two and zero propagating waves, respectively. A thick enough sample gives total reflection within the black regions and selective reflection within the gray regions. To discuss the origin and the meaning of the instability regions we must consider the following facts. 1) The coefficients a and b in Eq.6, and consequently the effective wavevectors k_j, are periodic function of ϕ, with period 2π. For any $\Delta\varphi$-value we have therefore an infinite number of instability regions, corresponding to l_b intervals with the same ϕ (modulus 2π) whose thickness linearly increases as the optical anisotropy Δn. 2) The angle $\Delta\varphi$ is defined modulus π, since it gives the direction of the optic axis of the layers.

Let us now consider the instability regions ① and ② where $\Delta\varphi \to 0$ and $\phi \to 0$. Since in these limits we obtain a uniform rotation of the optic axis, the considered instability regions are the extrapolation to the TGB phases of the well known Bragg reflection band of cholesterics at normal incidence.

Obviously the two regions correspond to helical structure with opposite handedness.

The third reflection band (③), independent of the polarization state, occurs around $\phi=\pi$, and is evidently due to the fact that the waves reflected by any couple of boundary planes add coherently. It corresponds to the Bragg reflection of a medium of period l_b, when the optical path along one period is equal to half wavelength, despite the fact that here the period of the superstructure is different. If l_b is in the visible range, this property allows us to get the value of the slab thickness by an optical method.

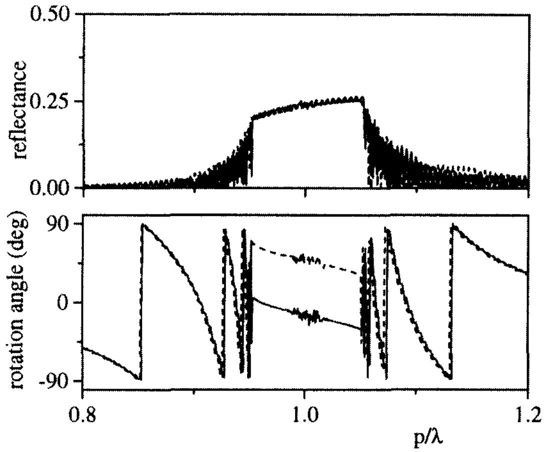

Fig 4: Reflection spectra and the optical rotation at normal incidence for two sample with $\Delta\varphi=18°$ and $\Delta\varphi=18.031415...°$. The other parameters are $n_e=1.66$, $n_o=1.5$ and $p=0.3\mu m$ and sample thickness $d=30\mu m$.

The separation lines between the different regions of the stability chart are continuous function of $\Delta\varphi$. This fact appears as rather strange, if we consider that the period of the structure dramatically changes by slightly changing $\Delta\varphi$. By setting $\Delta\varphi=\pi/a$, it is in fact easily understood that the period is al_b if a is an integer, it is greater if a is a rational number and it goes to infinite for irrational values of a (incommensurate phase). The position of the reflection band and the actual period of the structure are fully unrelated quantities. The point is that the reflection bands occur where k_j has an imaginary part. This part can be found (and is indeed computed) by making use of a rotating reference frame, as usual for helical structure. In this frame the medium appears in any case as periodic with period l_b. In the laboratory frame the real part of k_j and the corresponding eigenvectors are changed. This fact suggest that some other optical properties could be more sensitive to a small $\Delta\varphi$-change. We have considered the optical rotation through the sample and found that within a selective reflection band this quantity strongly depend on $\Delta\varphi$, as shown by Fig.4. The upper curves give the reflectance of the samples between parallel polarizers. The lower ones give the angle between the polarization direction of the linearly polarized input beam and the direction of the main axis of the output beam which is elliptically polarized.

OBLIQUE INCIDENCE.

The previous analysis is not allowed for oblique incidence because the propagation matrices U_n of the slab are different. The transfer matrix of the β vector for the whole sample is $U = U_N \times U_{N-1} \times ... \times U_1$. An analytical solution of the secular equation of the U-matrix does not exist and the four complex eigenvalues u_j of U are found numerically. If $|u_j|>1$ and $|u_j|<1$ the wave is evanescent increasing and decreasing, respectively, and if $|u_j|=1$ the wave is propagating.

Fig.3 shows the chart of stability for a TGBA sample as a function of p/λ (p is the pitch) and $p_0^2 = n_i^2 \sin^2\theta_i$, where n_i and θ_i are the refraction index and the incident angle within the external medium, respectively. This chart is very similar to the one found for cholesteric [12]. In particular, if the incidence angle goes to zero only the first order reflection band survives. Since the p/λ range in Fig.3 corresponds to $\phi<\pi/2$ only one of the bands given in Fig.2 appears.

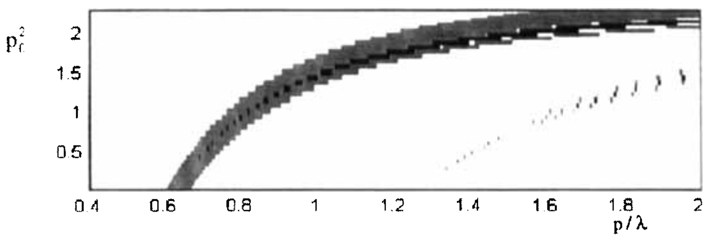

Fig.3 : Chart of stability for a TGBA sample with $\Delta\varphi=\pi/10$ $n_e=1.66$, $n_o=1.5$ and $n_i=1.5$, sample thickness $d=3\mu m$ as a function of p/λ and p_0^2,. Same legend as in Fig.2.

HOMOGENEOUS MODEL.

The TGB phases having a pitch shorter than the light wavelength can be approximated, for what concerns their optical properties, by an effective homogeneous medium characterized by a permittivity tensor and a gyration pseudo tensor. This homogeneous model is particularly useful to evidence the possible optical activity of the medium. Let summarize the main steps required to define the model. The Berreman matrix B(z) appearing in Eq.1 depends on z through the angle φ that defines the direction of the optic axis.

We first find out a constant Berreman matrix $\tilde{B}$ such that its transfer matrix $\tilde{U}$ for sample of thickness p (p is the pitch of the TGB sample, assumed as periodic) better approximates the transfer matrix U of a TGB sample with the same thickness. This is formally done by writing the stairs-like function $\varphi(z)$ as follow:

$$\varphi = qz + \Delta\varphi\left[\sum_{j=1}^{\infty}\frac{\sin\left(\frac{2\pi jqz}{\Delta\varphi}\right)}{j\pi} - \frac{1}{2}\right] + \varphi_0 . \qquad (7)$$

The Berreman matrix then is written as

$$B(z) = B_0 + \sum_{n=1}^{\infty}\sum_{m=0}^{\infty}\left[B_{nm}^{c+}\cos\left(k_{nm}^{+}qz\right) + B_{nm}^{c-}\cos\left(k_{nm}^{-}qz\right) + B_{nm}^{s+}\sin\left(k_{nm}^{+}qz\right) + B_{nm}^{s-}\sin\left(k_{nm}^{-}qz\right)\right] \qquad (8)$$

where $k_{nm}^{+} = m\frac{2\pi}{\Delta\varphi} + n$, $k_{nm}^{-} = m\frac{2\pi}{\Delta\varphi} - n$.

The expressions of the matrices B_0, B_{nm}^{c+}, ..., appearing in Eq.8 are rather complicated and are not given here. From the Eq.8, the properties of the homogeneous model are straightforwardly obtained [13,14]. The effective medium is uniaxial and non chiral except for small gyration terms scaling as $(p/\lambda)^3$, which are negligible to any practical purpose. The optic axis of the medium is along z and the principal values of the dielectric tensor are $\tilde{\varepsilon}_e = \varepsilon_o$, and $\tilde{\varepsilon}_o = (\varepsilon_o + \varepsilon_e)/2$. These optical properties are similar to the ones of the cholesteric phase.

CONCLUSIONS.

In this paper, we have studied some optical properties of the experimentally discovered TGB phases which are optically equivalent to the TGBA phase. We have analyzed the reflection bands at normal and oblique incidence by making use of stability charts. We have found that the position of the reflection bands does not depend on the actual period of the structure and is the same for commensurate and incommensurate structures, since the boundaries of the bands are a continuous and smooth function of the material parameters $\Delta\varphi$ and l_b. However, we have shown that, with a very fine analysis of the reflection bands, we can get the structural parameters of the TGBA phases. Analogies and differences between TGB and cholesteric phases have been evidenced. In particular, we have shown that the analogy is particularly strong for the optical rotation within short pitch samples.

The TGBA phases can present incommensurate structures [4]. For these structures it is generally not possible to define the periodicity of the medium and our homogeneous model can not be applied. The problem of the definition of an homogeneous model for non periodic medium is not reserved to liquid crystals but exists also in crystals [15]. Then, the one dimensional structure of these chiral liquid crystals can be helpful to understand the consequence of the incommensurability.

References

[1] P.G. de Gennes, *Solid State Commun*, **10,** 753 (1972).
[2] S.R. Renn, T.C. Lubensky, *Phys. Rev. A* **38,** 2132 (1988), T. C. Lubensky, S. R. Renn, *Phys. Rev. A* **41**, 4392 (1990).
[3] S.R. Renn, *Phys. Rev. A* **45,** 953 (1992).
[4] J.W. Goodby *& al, Nature* **337,** 449 (1989).
[5] L. Navaille, P. Barois, H.T. Nguyen, *Phys. Rev. Lett.* **71,** 545 (1993).
[6] P.A. Pramod, R. Pratibha and N.V. Madhusudana, *Current Science* **73,** 761 (1997).
[7] K.J. Ihn *& al, Science* **258,** 275 (1992).
[8] M. Petit, P. Barois and H.T. Nguyen, *Europhys. Lett.* **36,** 185 (1996).
[9] D.W. Berreman, *J. Opt. Soc. Am.* **62,** 502 (1972).
[10] C. Oldano, *Phys. Rev. A* **40,** 6014 (1989).
[11] G. Joly and J. Billard, *J. Optics (Paris)* **13**, 227 (1982).
[12] C. Oldano, *Phys. Rev. A* **27,** 3291 (1983).
[13] C. Oldano and M. Rajteri, *Phys. Rev. B* **54,** 10273 (1996).
[14] M. Becchi, P. Hubert, P. Jägemalm and C. Oldano, *ILCC"98.*
[15] J. Ortega *& al,. Phys. Rev. B* **45,** 5155 (1992).